

## Porewater-derived nutrient fluxes in a coastal aquifer (Shengsi Island, China) and its implication

Xiaogang Chen<sup>a</sup>, Jinlong Wang<sup>a</sup>, Neven Cukrov<sup>b</sup>, Jinzhou Du<sup>a,\*</sup>

<sup>a</sup> State Key Laboratory of Estuarine and Coastal Research, East China Normal University, Shanghai, 200062, China

<sup>b</sup> Division for Marine and Environmental Research, Ruder Bošković Institute, Zagreb, 10000, Croatia



### ARTICLE INFO

#### Keywords:

Porewater exchange  
 $^{222}\text{Rn}$  advection-diffusion model  
 Coastal aquifer  
 Silicon flux  
 Harmful algal blooms  
 Yangtze River Estuary

### ABSTRACT

As an important component of the hydrological and biogeochemical cycle, porewater discharge represents a significant pathway for releasing chemical solutes into coastal zones, particularly in highly permeable aquifers. In this study, a  $^{222}\text{Rn}$  advection-diffusion model was used to estimate the porewater discharge in a coastal aquifer (Shengsi Island, East China Sea) during November 2015. Porewater discharge was estimated to range from 7.4 to 25.8 (mean:  $12.9 \pm 5.8$ )  $\text{cm d}^{-1}$ . Furthermore, the estimated porewater-derived nutrient fluxes (dissolved inorganic nitrogen (DIN), phosphorus (DIP) and silicon (DSi)) ( $\text{mol m}^{-2} \text{ d}^{-1}$ ) were  $(1.7 \pm 1.4) \times 10^{-2}$ ,  $(2.1 \pm 1.1) \times 10^{-4}$  and  $(1.5 \pm 1.3) \times 10^{-2}$ , respectively. The Si/N ratio of coastal seawater at Shengsi Island was  $\sim 0.83$ , which is close to that of porewater along the coastal aquifers of Shengsi Island ( $\sim 0.92$ ) but higher than that of the Yangtze River Estuary ( $\sim 0.68$ ). Thus, porewater-derived Si flux with a higher Si/N ratio may mitigate the outbreak of non-siliceous algae (i.e., *Protorcentrum dentatum*) in adjacent waters of Shengsi Island. By comparing the SGD-derived nutrient fluxes worldwide, this study suggests that Si flux with a higher Si/N ratio through porewater discharge (or SGD) may strongly influence the Si budget and cycling because such porewater/SGD-derived Si can compensate for the dwindling Si flux from riverine sources due to human activity (i.e., dam construction, reservoirs). Our results are expected to increase our understanding of not only biogenic elements of cycling processes but also eco-environment processes such as the occurrences of harmful algal blooms alone river-influenced coasts.

### 1. Introduction

Submarine groundwater discharge (SGD) is defined as all the fluid flow on continental margins from the seabed to the coastal ocean, with scale lengths of meters to kilometres, regardless of the fluid composition and driving force (Burnett et al., 2003; Moore, 2010), which includes fresh groundwater discharge and recirculated seawater discharge (Taniguchi et al., 2002; Burnett et al., 2003; Santos et al., 2012). While the fresh groundwater discharge is a net source of dissolved species, the recirculated seawater discharge can either remove or add dissolved elements to seawater (Santos et al., 2011). Groundwater is synonymous with porewater in saturated sediments; thus, porewater discharge is generally thought to be one part of SGD (Moore, 2010; O'Reilly et al., 2015). Recent studies have shown the significance of porewater discharge as one of the most important vectors for the transport of nutrients, carbon, greenhouse gases and metals to coastal waters (Charette and Sholkovitz, 2006; Faber et al., 2014; Santos et al.,

2015; O'Reilly et al., 2015; Tait et al., 2017). The porewater discharge not only participates in the hydrological cycle but also affects marine systems by exporting nutrients and pollutants to coastal waters. Some studies regarding porewater discharge or SGD have focused on the associated deleterious effects on marine ecological environments, such as macro-algal eutrophication (Hwang et al., 2005a), red tides (Luo and Jiao, 2016), green tide blooms (Liu et al., 2017) and hypoxia formation (McCoy et al., 2011; Dale et al., 2013).

Groundwater is generally enriched in nutrients due to the natural processes or residential and agricultural development in near-shore areas, and even a small net SGD flux may deliver a comparatively large quantity of nutrients to coastal waters (Valiela et al., 1990; Boehm et al., 2006). Recent studies have found that the global mean discharge-weighted dissolved silicon (DSi) concentration of rivers is estimated to be  $158 \mu\text{mol L}^{-1}$  (Dürr et al., 2011), which is significantly lower than the global value estimated in the 1980s ( $173 \mu\text{mol L}^{-1}$ ) (Meybeck and Helmer, 1989). The coastal ecology is likely to continue toward silicon

\* Corresponding author. East China Normal University, State Key Laboratory of Estuarine and Coastal Research, 3663 North Zhongshan Road, SKLEC Building, Room 410, Shanghai, 200062, China.

E-mail address: [jzdu@sklec.ecnu.edu.cn](mailto:jzdu@sklec.ecnu.edu.cn) (J. Du).

limitation and primary production dominated by non-siliceous algae, especially in some estuarine areas (Tréguer and De La Rocha, 2013). However, the effect of the SGD-derived Si flux on the ecological environment in some river-influenced regions under the background of dramatically decreased Si input from rivers (e.g., Yangtze River, Nile River and Danube River) has not received enough attention (Dai et al., 2010; Wahby and Bishara, 1981; Teodoru et al., 2006; Humborg et al., 2000). Meanwhile, several studies have found that SGD appears to be an important source of silicon and has a significant impact on the global ocean silicon budget (Kim et al., 2005; Georg et al., 2009). Therefore, the Si flux conveyed by SGD should be given enough attention under the background of global Si decline from rivers, especially in river-influenced regions.

The Yangtze River had a huge runoff and sediment load, annually  $9.2 \times 10^{11} \text{ m}^3$  and  $4.8 \times 10^8 \text{ t}$ , respectively, before 2000 (Yang et al., 2006). However, the sediment load has recently exhibited an obvious decreasing tendency in the Yangtze River (from  $3.5 \times 10^8 \text{ t yr}^{-1}$  in 2000 to  $2.0 \times 10^8 \text{ t yr}^{-1}$  in 2011) (Yang et al., 2005; Dai and Liu, 2013). In the past 50 years, Dai et al. (2010) reported that there was a sharp decrease in the Si/N ratio and an increase in the N/P ratio, which was likely to cause the increase of red tide blooms and a decrease of dissolved oxygen in the Yangtze River Estuary. Generally, the groundwater contains high concentrations of nutrients, and the proportions of groundwater nutrients are different from the Redfield-Brzezinski proportions (Si:N:P = 15:16:1), which may have a significant effect on coastal ecosystems by influencing the community composition of phytoplankton (Lee et al., 2010; Su et al., 2011). Radon ( $^{222}\text{Rn}$ , half-life 3.82 days) has been considered to be an excellent porewater discharge tracer since it is often naturally enriched in porewater, behaves conservatively as a noble gas, is relatively easy to measure, and its short half-life can match the oceanographic processes of a time scale of 1–20 days (Burnett and Dulaiova, 2006; Santos et al., 2015). In this study, to calculate porewater discharge from aquifers to coastal ecosystems, a  $^{222}\text{Rn}$  advection-diffusion model was constructed. The objective of this work is to estimate the porewater discharge and the associated nutrient fluxes in a coastal aquifer (Shengsi Island, China) and to evaluate the eco-environmental impacts on coastal ecosystems.

## 2. Materials and methods

### 2.1. Study area

Shengsi Island is located in the west of the East China Sea (ECS) and is close to the Yangtze River Estuary (Fig. 1a). It belongs to a subtropical maritime monsoon climate, with an annual mean temperature

of  $16^\circ\text{C}$  and mean annual rainfall of 1106 mm (<http://data.cma.cn>). Shengsi is composed by 404 islands, covers a total area of  $8824 \text{ km}^2$ , and the land area is  $88 \text{ km}^2$  (Chen et al., 2015). Serving as one of the ten largest fishing counties in China, the aquatic resources of Shengsi Island located in the centre of the famous Zhoushan Fishing Ground are very rich. During recent years, the neighbouring waters of Shengsi Island suffer from the frequent occurrence of red tides, such as the outbreaks of non-siliceous algae (*Prorocentrum dentatum*) rather than siliceous algae (*Skeletonema costatum*) (Zhang and Yu, 2001; Liu et al., 2016).

### 2.2. Field sampling and laboratory analysis

The field observations were performed at Shengsi Island during November 2015. The porewater samples from a highly permeable aquifer of the offshore zone were collected by using a push-point piezometer and a peristaltic pump (Charette and Allen, 2006). The porewater profiles were collected at stations P1, P2, P3, P4, P5, P10 and P12 (Fig. 1b). Salinity and temperature were measured in situ using a YSI-EC300A conductivity meter. To prevent bubbles and avoid losses via atmospheric exchange during sampling,  $^{222}\text{Rn}$  samples ( $n = 50$ ) were slowly collected (approximately  $0.5 \text{ L min}^{-1}$ ) into a RAD7-H<sub>2</sub>O 250 mL sample bottle with the overflow method (Wen et al., 2014; Chen et al., 2018a,b) and immediately analysed by a RAD7 detector (Durridge Co., Inc., USA) according to the manufacturer's instructions. Nutrient samples ( $n = 7$ ) were filtered by the  $0.45 \mu\text{m}$  cellulose acetate filters that was pre-cleaned with hydrochloric acid and rinsed with Milli-Q water and were filled into polyethylene bottles. Then, the samples were poisoned with saturated  $\text{HgCl}_2$  and were kept away from the light until the laboratory measurement. The nutrient concentrations ( $\text{NO}_2^-$ ,  $\text{NO}_3^-$ ,  $\text{NH}_4^+$ ,  $\text{PO}_4^{3-}$  and  $\text{SiO}_3^{2-}$ ) were determined using an auto-analyser (Model: Skalar SANplus146) (Liu et al., 2005, 2009). The DIP and DSi are the concentrations of  $\text{PO}_4^{3-}$  and  $\text{SiO}_3^{2-}$ , respectively. The DIN represents the sum of  $\text{NO}_2^-$ ,  $\text{NO}_3^-$  and  $\text{NH}_4^+$ . A sediment equilibration experiment was performed to estimate the amount of porewater  $^{222}\text{Rn}$  at equilibrium with the solid phase sediments. Each wet sediment sample (approximately 100 g) was sealed in an Erlenmeyer flask with approximately 400–500 mL of seawater for 20–30 days. After this period, the equilibrium activity ( $C_{eq}$ ) was calculated using the porosity ( $\varphi$ ) and wet bulk density ( $\rho_{wet}$ ) of the sediments (Cable et al., 1996).

### 2.3. Modelling

The groundwater flows transport water, solutes and particles from permeable aquifers to the coastal ocean, and these waters mix prior to discharging and form a porewater-seawater mixing zone (Fig. 2a)

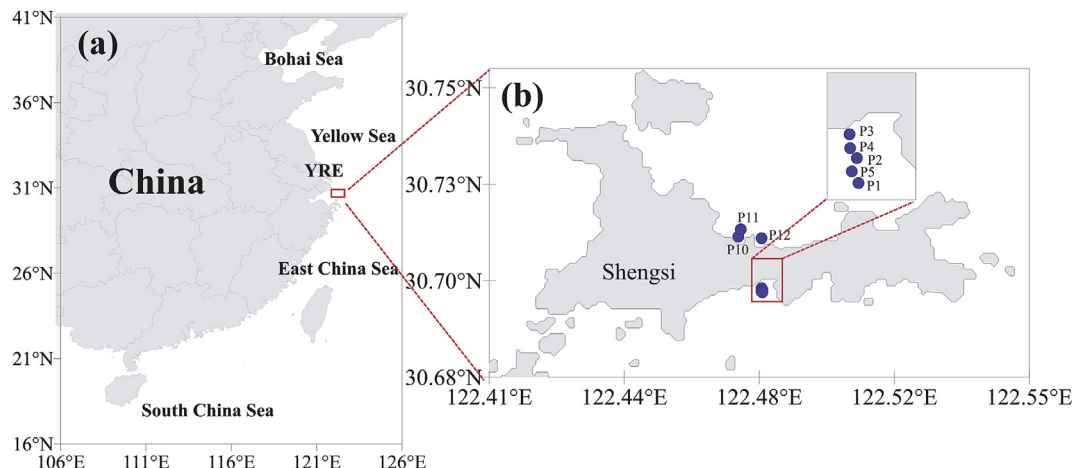


**Fig. 1.** Map showing the study sites. Blue dots represent porewater stations (YRE: Yangtze River Estuary). (For interpretation of the references to colour in this figure legend, the reader is referred to the Web version of this article.)

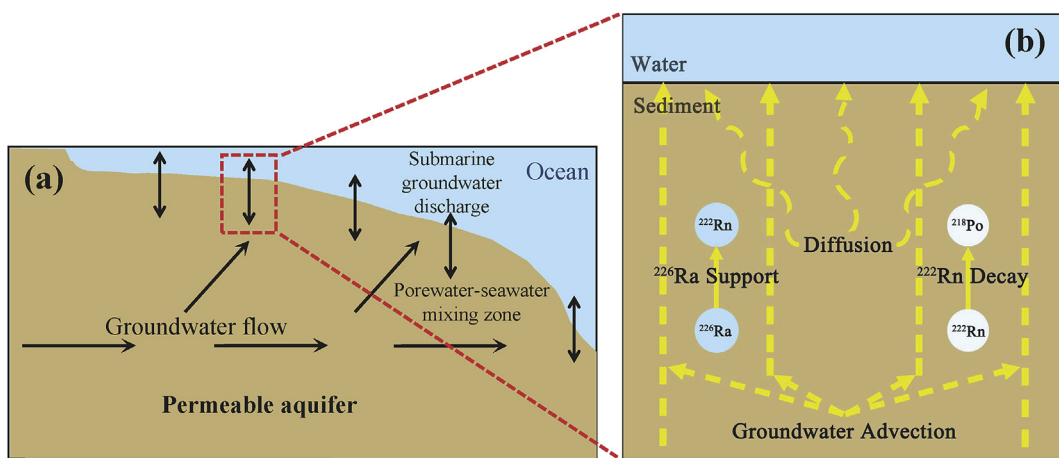


**Fig. 2.** (a) Conceptual model of the groundwater flow and porewater-seawater interface in a beach aquifer. (b) Schematic diagram of the  $^{222}\text{Rn}$  advection-diffusion model describing the various processes that occur in the aquifer system (Smith et al., 2008).

(Smith et al., 2008). In the aquatic system (Fig. 2b), there are a few factors can contribute to the  $^{222}\text{Rn}$  profile in depth; diffusive fluxes from sediment can contribute  $^{222}\text{Rn}$  to overlying waters and advective processes can greatly increase the input of  $^{222}\text{Rn}$ . Meanwhile, the  $^{222}\text{Rn}$  advection-diffusion process also involves the decay of  $^{222}\text{Rn}$  and the contribution of  $^{226}\text{Ra}$  present in the wet sediment. Irrigation is a non-local exchange of a dissolved constituent between porewater and the overlying water (Smith et al., 2008). If salinity does not vary with depth or changes very little in the porewater profile, irrigation is usually neglected. Thus, the advection-diffusion equation can be obtained by the following equation (Craig, 1969; Benoit et al., 1991; Cable et al., 1996):

$$\frac{\partial C}{\partial t} = \left( D_s \frac{\partial^2 C}{\partial z^2} + \lambda P \right) - \left( \nu \frac{\partial C}{\partial z} + \lambda C \right) \quad (1)$$

where  $C$  is the  $^{222}\text{Rn}$  activity in the porewater ( $\text{Bq m}^{-3}$ );  $t$  is time (d);  $z$  is the depth below the sediment-water interface (positive downward) (cm);  $D_s$  is the bulk sedimentary diffusion coefficient ( $\text{cm}^2 \text{ d}^{-1}$ );  $\nu$  is the advective velocity (i.e., porewater discharge rate) ( $\text{cm d}^{-1}$ );  $P$  is the  $^{222}\text{Rn}$  activity ( $\text{Bq m}^{-3}$ ) emanating from the sediments and determined by sediment equilibration experiments (Martens et al., 1980; Cable et al., 1996); and  $\lambda$  is the decay constant of  $^{222}\text{Rn}$  ( $0.181 \text{ d}^{-1}$ ).

The wet bulk sedimentary diffusion coefficient can be approximately obtained by the product of porosity ( $\varphi$ ) and the molecular diffusivity coefficient ( $D_o$ ) of  $^{222}\text{Rn}$  (Peng et al., 1974; Ullman and Aller, 1982):

$$D_s \approx \varphi D_o \quad (2)$$

$$D_o = 10^{-\left[ \left( \frac{980}{T+273} \right) + 1.59 \right]} \quad (3)$$

where  $T$  ( $^\circ\text{C}$ ) is the temperature of the porewater.

In Eq. (1), assuming a steady state is available, i.e.,  $\frac{\partial C}{\partial t} = 0$ , with boundary conditions:  $C(z=0) = C_0$  and  $\left. \frac{dC}{dz} \right|_{z=z_{eq}} = 0$ , the analytical solution of Eq. (1) can be obtained as (Cable et al., 1996):

$$C = \frac{(C_0 - C_{eq}) \left( e^{\frac{z}{z^*}} \right) \sinh \left( \frac{A(z_{eq}-z)}{2z^*} \right)}{\sinh \left( \frac{Az_{eq}}{2z^*} \right)} + C_{eq} \quad (4)$$

in which  $z^*$  is a one-dimensional mixing parameter ( $z^* = \frac{D_s}{\nu}$ );  $A = (1 - 4z^*)(\lambda/\nu)^{0.5}$ , which includes radioactive decay and advection (Martens et al., 1980);  $C_{eq}$  is the equilibrated  $^{222}\text{Rn}$  activity ( $\text{Bq m}^{-3}$ ) at depth layer  $z_{eq}$  (cm) in the sediments;  $z_{eq}$  is a depth much deeper than the depth at which  $C_{eq}$  initially occurs; and  $C_0$  is the overlying  $^{222}\text{Rn}$

activity of bottom water ( $\text{Bq m}^{-3}$ ).

Using the  $^{222}\text{Rn}$  activity in the groundwater end-member entering the system ( $C_{gw}$ ,  $\text{Bq m}^{-3}$ ) and porewater discharge rate of  $^{222}\text{Rn}$  ( $\nu$ ,  $\text{cm d}^{-1}$ ), the advective flux (i.e., porewater discharge flux) ( $F_{adv}$ ,  $\text{Bq m}^{-2} \text{ d}^{-1}$ ) could be converted by:

$$F_{adv} = \nu C_{gw} \quad (5)$$

In addition, diffusion-exchange across the sediment-water interface would occur when the activity of  $^{222}\text{Rn}$  in the porewater is higher than that in the overlying water. The  $^{222}\text{Rn}$  diffusive flux across the sediment-water interface is described by Martens et al. (1980):

$$F_{diff} = (\lambda D_s)^{0.5} (C_{eq} - C_o) \quad (6)$$

where  $F_{diff}$  is the diffusive  $^{222}\text{Rn}$  flux of radon from the sediments ( $\text{Bq m}^{-2} \text{ d}^{-1}$ ). The  $\lambda$ ,  $D_s$ ,  $C_{eq}$  and  $C_o$  are explained previously.

### 3. Results

#### 3.1. Hydrographic and geochemical properties in coastal aquifer

The porewater profiles of  $^{222}\text{Rn}$  activity, salinity and temperature are shown in Fig. 3. The porewater temperatures ( $^\circ\text{C}$ ) and salinity in the coastal aquifer of Shengsi Island ranged from 15.9 to 24.3 and 0.1 to 26.9, respectively. The porosity of the sediment changed from 0.27 to 0.34. The  $^{222}\text{Rn}$  activity significantly increased from the surface to the bottom layer of water profiles, which was reversed with the variation trend of salinity profiles. Since the change of porewater temperature lags relatively behind the air temperature, the temperature of porewater regularly decreases or increases with water depth. Overall, the variation of porewater salinity and temperature are relatively smaller compared to the  $^{222}\text{Rn}$  activity.

#### 3.2. $^{222}\text{Rn}$ and nutrients in porewater end-members

At deeper depths (50–120 cm below sea floor) of each porewater profile,  $^{222}\text{Rn}$  activities almost did not change with depths because of near equilibrium (Fig. 3). We used the porewater samples at the equilibrium depths as the porewater end-members. The  $^{222}\text{Rn}$ , nutrients, salinity and temperature in porewater end-members of Shengsi Island are shown in Table 1. The temperature ( $^\circ\text{C}$ ) in porewater end-members varied from 17.3 to 20.8. The salinity varied over a large magnitude in the porewater end-members, with values from 0.1 to 23.8. The  $^{222}\text{Rn}$  activity in the porewater end-members varied from  $(2.07 \pm 0.26) \times 10^3$  to  $(11.1 \pm 0.50) \times 10^3$  (mean:  $(5.25 \pm 2.79) \times 10^3 \text{ Bq m}^{-3}$ , which were much higher than those in the coastal seawater ( $181 \pm 69.2 \text{ Bq m}^{-3}$ ). The concentrations of the

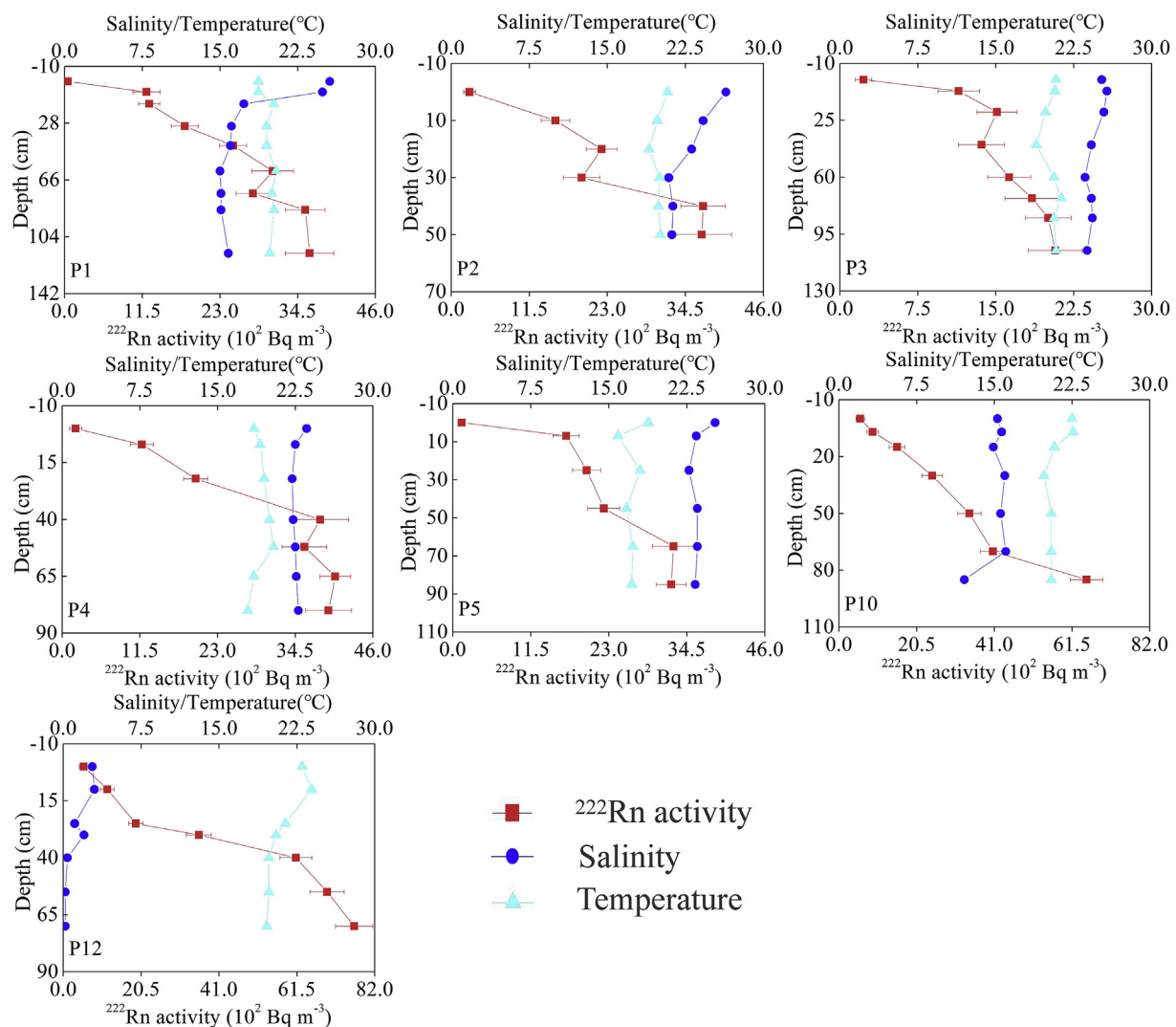


**Fig. 3.** Porewater profiles of measured  $^{222}\text{Rn}$  activities (red squares), salinity (blue dots) and temperature (cyan triangles). (For interpretation of the references to colour in this figure legend, the reader is referred to the Web version of this article.)

DIN, DIP and DSi in porewater end-members varied from 22.4 to 347 (mean:  $129 \pm 94$ )  $\mu\text{mol L}^{-1}$ , 1.08 to 2.24 (mean:  $1.60 \pm 0.41$ )  $\mu\text{mol L}^{-1}$  and 67.4 to 320 (mean:  $119 \pm 85$ )  $\mu\text{mol L}^{-1}$ , respectively. The mean concentrations of DIN, DIP and DSi in the coastal seawater of Shengsi Island were  $59.8 \pm 10.9$   $\mu\text{mol L}^{-1}$ ,  $1.52 \pm 0.32$   $\mu\text{mol L}^{-1}$  and  $49.7 \pm 2.1$   $\mu\text{mol L}^{-1}$ , respectively, and they were all significantly lower than those in porewater end-members. The mean Si/N ratio of

coastal seawater at Shengsi Island was  $\sim 0.83$  and this is close to those of porewater end-members (0.92). Moreover, the mean Si/N ratio ( $\sim 0.92$ ) in the porewater end-members was close to the Redfield-Brzezinski Si/N ratio (15:16). Higher  $^{222}\text{Rn}$  activities and DIP and DSi concentrations were observed in the porewater end-members with lower salinity, and the lower level occurred in high salinity (Fig. 4a, c, d), but the DIN had no obvious correction with salinity in the porewater

**Table 1**

Summary of temperature, salinity,  $^{222}\text{Rn}$  activity, nutrient concentrations (DIN, DIP and DSi) and the Si/N ratio for porewater end-members.

Station	Longitude	Latitude	Temperature	Salinity	$^{222}\text{Rn}$ activity	DIN	DIP	DSi	Si/N ratio
	°E	°N	°C		Bq m <sup>-3</sup>	μmol L <sup>-1</sup>	μmol L <sup>-1</sup>	μmol L <sup>-1</sup>	
P1	122.4824	30.7014	19.8	15.8	$3630 \pm 360$	347	2.24	130	0.37
P2	122.4823	30.7015	19.9	21.3	$3710 \pm 330$	116	1.31	77.7	0.67
P3	122.4821	30.7016	20.8	23.8	$2070 \pm 260$	92.2	1.08	67.4	0.73
P4	122.4822	30.7015	18.5	22.6	$4040 \pm 230$	95.2	1.26	67.7	0.72
P5	122.4823	30.7014	17.3	23.5	$3250 \pm 310$	118	1.90	89.2	0.75
P10	122.4752	30.7135	20.5	12.1	$6530 \pm 430$	22.4	1.38	77.8	3.55
P11	122.4751	30.7138	20.3	0.1	$11100 \pm 500$	nd <sup>a</sup>	nd	nd	nd
P12	122.4779	30.7123	19.6	0.2	$7660 \pm 490$	111	2.03	320	2.88
Mean			19.6	14.9	5250	129	1.60	119	0.92
Std. dev.			1.1	9.3	2790	94	0.41	85	1.17

<sup>a</sup> Not determined.

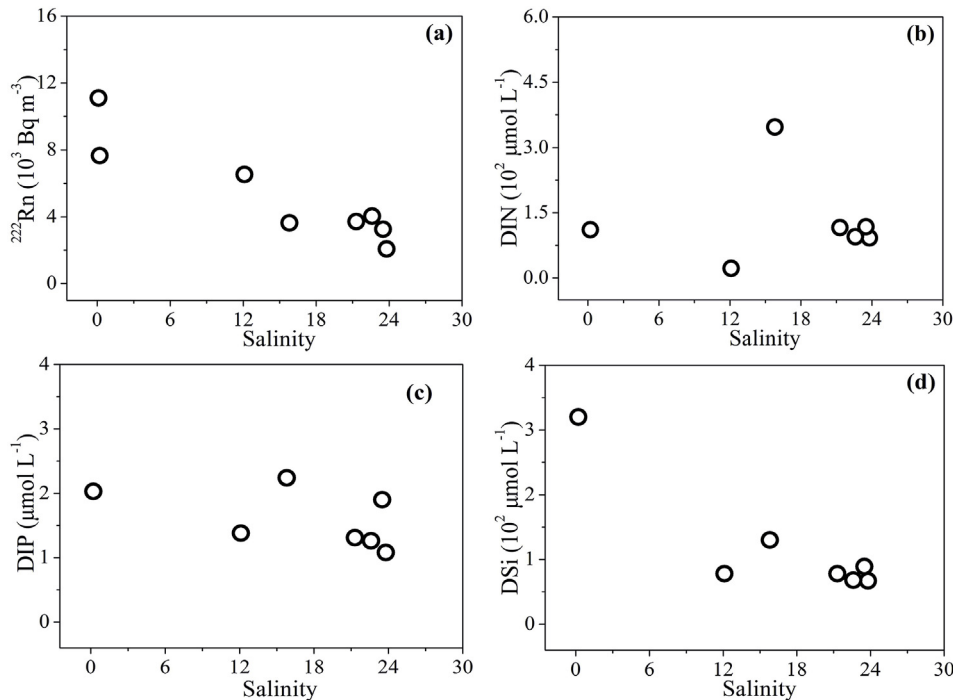


Fig. 4. Plots of  $^{222}\text{Rn}$ , DIN, DIP and DSi versus salinity in porewater end-members of Shengsi Island.

end-members (Fig. 4b).

#### 4. Discussions

##### 4.1. Porewater discharge traced by $^{222}\text{Rn}$ advection-diffusion model

Based on the  $^{222}\text{Rn}$  advection-diffusion model (Eqs. (1) and (4)), the substituted parameters (including  $C$  ( $\text{Bq m}^{-3}$ ),  $z$  (cm),  $T$  ( $^\circ\text{C}$ ),  $z_{eq}$  (cm),  $\lambda$  ( $\text{d}^{-1}$ ),  $D_s$  ( $\text{cm}^2 \text{ d}^{-1}$ ),  $\varphi$ ,  $C_o$  ( $\text{Bq m}^{-3}$ ) and  $C_{eq}$  ( $\text{Bq m}^{-3}$ )) were used to calculate the porewater discharge rate (Table 2). The porewater discharge rates on Shengsi Island were estimated to range from 7.4 to 25.8 (mean:  $12.9 \pm 5.8$ )  $\text{cm d}^{-1}$  (Table 2). The maximum value of porewater discharge appears at station P3, which is the nearest offshore station (Fig. 1). Then, the porewater discharge flux can be obtained by the product of the porewater discharge rate and the  $^{222}\text{Rn}$  activity in the porewater. Based on this, we obtained porewater discharge fluxes ranging from 390 to 1400 (mean:  $680 \pm 470$ )  $\text{Bq m}^{-2} \text{ d}^{-1}$ . Note that the major fraction of porewater discharge is recirculated water.

From Eqs. (2) and (3), the  $D_s$  were calculated to be  $0.31 \pm 0.03$ – $0.32 \pm 0.02 \text{ cm}^2 \text{ d}^{-1}$  (mean:  $0.32 \pm 0.01 \text{ cm}^2 \text{ d}^{-1}$ ). The equilibrated  $^{222}\text{Rn}$  activity ( $C_{eq}$ ) was determined by a sediment equilibration experiment (Cable et al., 1996), which ranged between 5000 and 7900  $\text{Bq m}^{-3}$  (mean:  $6600 \pm 1200 \text{ Bq m}^{-3}$ ). The  $C_o$  ranged

between  $227 \pm 40$  and  $538 \pm 60 \text{ Bq m}^{-3}$  (mean:  $443 \pm 153 \text{ Bq m}^{-3}$ ). Based on Eq. (6), the  $^{222}\text{Rn}$  diffusive fluxes were calculated to range from  $11.6 \pm 4.2$  to  $17.5 \pm 2.5 \text{ Bq m}^{-2} \text{ d}^{-1}$  (mean:  $14.7 \pm 3.0 \text{ Bq m}^{-2} \text{ d}^{-1}$ ) in the sediment-water interface of Shengsi Island. The  $^{222}\text{Rn}$  advective fluxes (i.e., porewater discharge fluxes,  $680 \pm 470 \text{ Bq m}^{-2} \text{ d}^{-1}$ ) were approximately 46 times the  $^{222}\text{Rn}$  diffusive fluxes, which indicated that the advective process is dominant relative to the diffusive process in the permeable aquifer.

##### 4.2. Porewater-derived nutrient fluxes

The nutrients are generally enriched in porewater as a result of the remineralization processes in saline groundwater (Slomp and Van Cappellen, 2004), and the recharge of water containing land-derived nutrients and the other pollutants into aquifers (Nolan et al., 2002). Porewater discharge is a significant pathway from land to coastal systems for nutrient fluxes (e.g., Slomp and Van Cappellen, 2004; Tait et al., 2017), which can lead to a range of effects on coastal ecosystems and significantly impact global nutrient cycling (Slomp and Van Cappellen, 2004). The nutrient fluxes from porewater discharge were determined by using the porewater discharge rate ( $12.9 \pm 5.8 \text{ cm d}^{-1}$  in this study) multiplied by the product of mean concentrations of nutrients in porewater end-members. Therefore, the porewater-derived

Table 2

Constant and fitted parameters (including the  $^{222}\text{Rn}$  activity of porewater ( $C$ ), the depth below the sediment-water interface ( $z$ ), temperature of porewater ( $T$ ), the depth much deeper than the depth where  $C_{eq}$  initially occurs ( $z_{eq}$ ), decay constant of  $^{222}\text{Rn}$  ( $\lambda$ ), sedimentary diffusion coefficient ( $D_s$ ), porosity ( $\varphi$ ),  $^{222}\text{Rn}$  activity of overlying water ( $C_o$ ) and equilibrated  $^{222}\text{Rn}$  activity at depth layer  $z_{eq}$  in the sediments ( $C_{eq}$ )) and porewater discharge ( $v$ ).

Station	$C$	$z$	$T$	$\varphi$	$C_o$	$z_{eq}$	$\lambda$	$C_{eq}$	$D_s$	$v$
	$\text{Bq m}^{-3}$	cm	$^\circ\text{C}$		$\text{Bq m}^{-3}$	cm	$\text{d}^{-1}$	$\text{Bq m}^{-3}$	$\text{cm}^2 \text{ d}^{-1}$	$\text{cm d}^{-1}$
P1	1210–3630	7–115	18.7–20.4	0.30–0.34	48	1000	0.181	5030	$0.32 \pm 0.04$	$12.1 \pm 3.8$
P2	1540–3710	10–50	19.0–20.8	0.30–0.34	270	1000	0.181	5030	$0.32 \pm 0.04$	$7.6 \pm 2.9$
P3	1140–2070	7–105	18.9–21.3	0.30–0.34	227	1000	0.181	5030	$0.32 \pm 0.04$	$25.8 \pm 12.2$
P4	1180–4040	7–80	17.9–20.4	0.30–0.34	200	1000	0.181	5030	$0.32 \pm 0.04$	$7.4 \pm 1.7$
P5	1670–3250	7–85	15.9–18.8	0.30–0.34	133	1000	0.181	5030	$0.32 \pm 0.04$	$10.9 \pm 4.8$
P10	892–6530	7–85	19.8–22.6	0.27–0.32	565	1000	0.181	6890	$0.32 \pm 0.02$	$15.2 \pm 5.9$
P12	1160–7660	10–70	19.6–23.9	0.29–0.31	538	1000	0.181	7910	$0.31 \pm 0.03$	$11.1 \pm 8.2$

**Table 3**  
Comparison of SGD and its derived-nutrient fluxes with previous studies in some coastal systems worldwide.

Study area	Tracer	$^{222}\text{Rn}$ activity in groundwater end-member	SGD rate	DIN flux	DIP flux	DSi flux	Si/N ratio	References
		Bq m <sup>-3</sup>	cm d <sup>-1</sup>	10 <sup>-3</sup> mol m <sup>-2</sup> d <sup>-1</sup>	10 <sup>-5</sup> mol m <sup>-2</sup> d <sup>-1</sup>	10 <sup>-3</sup> mol m <sup>-2</sup> d <sup>-1</sup>		
Bangdu Bay, Korea	$^{224,226}\text{Ra}$	242–1280 (mean: 820)	33–49	21	16	46	2.2	Hwang et al. (2005a)
Yeojia Bay, Korea	$^{223,224,226}\text{Ra}$	—	24	26	11	26	1.0	Hwang et al. (2005b)
Tampa Bay, USA	$^{223,224,226,228}\text{Ra}$	6320–107000 (mean: 63300)	0.22–1.5	0.13–0.87	1.9–14	0.87–6.0	6.7	Szwarczki et al. (2007)
Indian River Lagoon, USA	Seepage meter	—	2.7–6.4	0.06–0.07	0.27–0.44	0.14–0.34	2.3–4.9	Bhadha et al. (2007)
Obama Bay, Japan	$^{222}\text{Rn}$	3600–18600 (mean: 11000)	0.61	0.54	2.1	0.56	1.0	Sugimoto et al. (2016)
Geoje Bay, Korea	$^{222}\text{Rn}$	767–6420 (mean: 3400)	5.0	2.0	3.0	5.9	3.0	Hwang et al. (2016)
La Paz Bay, Mexico	$^{222}\text{Rn}$	417–8520 (mean: 3900)	10–18	2.0–52	4.0–94	7.0–160	4.8	Urquidi-Gaume et al. (2016)
Xiangshan Bay, China	$^{222}\text{Rn}$	1710–1740 (mean: 1730)	23–69	230–680	120–360	97–290	0.43	Wu et al. (2013)
Jiulong River Estuary, China	$^{226}\text{Ra}$	—	3.7–20	12–68	0.63–3.4	20–110	1.3	Wang et al. (2015)
Ladye Lagoon, China	$^{223,224,226,228}\text{Ra}$	—	9.4	3.3	89	1400	19 (well water)	Wang and Du (2016)
Xiaohai Lagoon, China	$^{223,224,226,228}\text{Ra}$	—	4.1	36	190	580	19	Wang and Du (2016)
Daya Bay, China	$^{222}\text{Rn}$	318–38300 (mean: 5100)	28–31	14	24	37	2.7	Wang et al. (2017)
Maowei Sea, China	$^{222}\text{Rn}$	1790–11500 (mean: 5100)	36	33	39	69.5	0.98	Chen et al. (2018a)
Shengsi Island, China	$^{222}\text{Rn}$	2070–11100 (mean: 5250)	12.9	17	21	15	0.92 (porewater)	This study

nutrient fluxes ( $\text{mol m}^{-2} \text{d}^{-1}$ ) (DIN, DIP and DSi) in Shengsi Island were estimated to be  $(1.7 \pm 1.4) \times 10^{-2}$ ,  $(2.1 \pm 1.1) \times 10^{-4}$  and  $(1.5 \pm 1.3) \times 10^{-2}$ , respectively. The nutrient fluxes (DIN, DIP and DSi) through the porewater discharge on Shengsi Island were in the range of global level (Table 3). Because there is no river discharge on Shengsi Island, atmospheric deposition serves as one of the sources of nutrients into coastal water. Zhang et al. (2007a,b) estimated the DIN, DIP and DSi fluxes from atmospheric deposition on Shengsi Island to be  $1.9 \times 10^{-4}$ ,  $3.1 \times 10^{-7}$  and  $5.2 \times 10^{-6} \text{ mol m}^{-2} \text{ d}^{-1}$ , respectively. We found that the fluxes of porewater-derived DIN, DIP and DSi into the coastal water on Shengsi Island were 2–4 magnitudes higher than those from atmospheric deposition, which implies that the porewater discharge serves as an important source of nutrients to coastal water at Shengsi Island.

#### 4.3. Effects of the porewater/SGD-derived Si flux on the coastal system

The DSi concentration and flux of the Yangtze River have decreased in the past 50 years, but the DIN and DIP concentrations and fluxes have increased, especially since the 1980s. The Si/N ratio of the Yangtze River Estuary has decreased from 6.23 in the 1960s to 0.68 in 2012 (Fig. 5). However, the N/P ratio of the Yangtze River Estuary had obvious fluctuations, with an increase from 84 during the 1960s to 154 during the 1970s, but with a decrease to 87 during the 2000s (Dai et al., 2010; Liu et al., 2016). The occurrences of red tides in the Yangtze River Estuary rapidly increased from 29 in the 1980s to 195 during 2000–2007 (Fig. 5). The increasing blooms in recent years are mainly non-siliceous algae (*Prorocentrum dentatum*) rather than siliceous algae (*Skeletonema costatum*) (Zhang et al., 2007a,b; Zhou et al., 2008; Liu et al., 2016). In present study area, the porewater discharge fluxes associated with its derived-nutrient fluxes (DIN, DIP and DSi) on Shengsi Island were in the range of the global level (Table 3). The mean Si/N ratio of porewater on Shengsi Island was 0.92, which was very closed to the requirements for phytoplankton growth (Si:N = 15:16), but it was higher than the Si/N ratio (~0.68) of the Yangtze River Estuary (Liu et al., 2016). The results of Wang et al. (2018) showed that mean Si/N ratio from groundwater was 2.18 along the coasts of ECS, which was much higher than the Si/N ratio (~0.68) of the Yangtze River Estuary (Liu et al., 2016). In addition, we found that the Si/N ratio in groundwater and porewater ranged from 0.43 to 19 in many cases, which were mostly higher than the Redfield-Brzezinski proportions (Si:N = 15:16) (Table 3). Therefore, the higher Si/N ratios in porewater (or groundwater) could be expected to affect coastal ecosystems by changing the microalgal community composition in coastal waters. In turn, this may weaken the occurrence of blooms of non-siliceous algae (i.e., *Prorocentrum dentatum*) in the Yangtze River Estuary. Meanwhile, Wang et al. (2018) estimated that SGD-derived DIN, DIP and DSi fluxes in the East China Sea were approximately 0.7, 2.2 and 1.4 times the Yangtze River input. In addition, regardless of flood season or dry season, Liu et al. (2018) found that SGD-derived nutrient fluxes appeared to be a major source of nutrient input into the Yangtze River Estuary, especially in the dry season. Thus, we imply that the porewater discharge (or SGD) may strongly influence the nutrient budget and cycling on Shengsi Island and in its adjacent waters such as Yangtze River Estuary, especially for Si.

Although our data are limited, the estimated SGD with a higher Si/N ratio and Si flux has significant effects on the coastal ecosystem in many research cases (Dollar and Atkinson, 1992; Kim et al., 2005; Georg et al., 2009). Based on the  $^{226}\text{Ra}$  mass balance model, Kim et al. (2005) evaluated the SGD flux to be at least 40% of the river-water input ( $\sim 2.3 \times 10^{11} \text{ m}^3 \text{ yr}^{-1}$ ) and the flux of Si through SGD to be 20%–100% of that associated with river discharge ( $\sim 23 \times 10^9 \text{ mol yr}^{-1}$ ) in the Yellow Sea, which implies that the Si flux through SGD may be significant on a global scale. Gu et al. (2012) found that the SGD flux was  $(0.2\text{--}1.0) \times 10^9 \text{ m}^3 \text{ d}^{-1}$  in the Yangtze River Estuary, and this was equivalent to 6%–30% of the Yangtze River water discharge during the

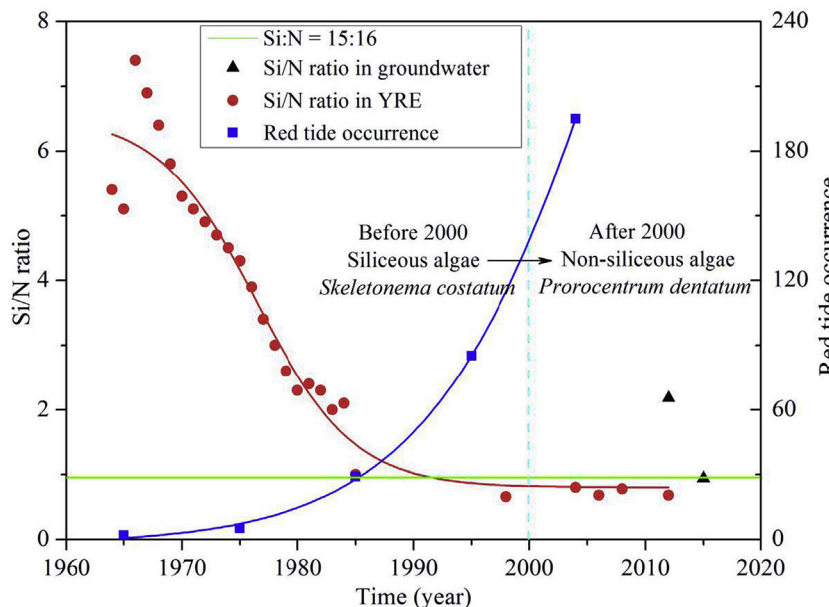


**Fig. 5.** Variations in the frequency of red tides and the Si/N ratio in the Yangtze River Estuary (YRE) (data from Dai et al., 2010 and Wang et al., 2016). The green line represents the Redfield-Brzezinski proportions (Si:N = 15:16), and the cyan dashed line represents the year 2000 as a boundary. The black triangles represent the Si/N ratio in the groundwater near the YRE (data from Wang et al. (2018) and this study). (For interpretation of the references to colour in this figure legend, the reader is referred to the Web version of this article.)

flood season, which indicates that SGD may also be important for the nutrient source in the ECS. The Si concentration and Si/N ratio play an important role in the control of phytoplankton primary production rates during the productive period, which can explain the spatial, seasonal and inter-annual variability of phytoplankton (Glé et al., 2008). However, in addition to the Yangtze River, the Si concentration and the Si/N ratio have been decreasing in many rivers worldwide, such as the Nile River (Wahby and Bishara, 1981), Danube River (Teodoru et al., 2006; Humborg et al., 2000) and Colorado River (Mayer and Gloss, 1980), etc. For example, the Si concentration of the Danube River was ca.  $140 \mu\text{mol L}^{-1}$  in the late 1950s (Cociasu et al., 1996), which is close to the world average of  $150 \mu\text{mol L}^{-1}$  (Tréguer et al., 1995), but it was only approximately  $58 \mu\text{M} \mu\text{mol L}^{-1}$  during 1979–1992 (Humborg et al., 1997). On a yearly basis, the Si load of the Danube River has been reduced by approximately 600,000 tons, and there are indications that the proportion of diatoms in the spring bloom has decreased while that of flagellates have increased (Humborg et al., 2000). However, the SGD-derived nutrients flux (including Si) is not available, which largely limits the understanding of the formation mechanism of blooms occurring in this region. Thus, the SGD-derived nutrient fluxes with higher Si/N ratios should be given adequate attention in these rivers and their adjacent waters. Previous studies suggested that SGD-derived nutrients can lead to outbreaks of red tides (e.g., Lee et al., 2010; Luo and Jiao, 2016). However, our study shows that a Si flux with a higher Si/N ratio through porewater discharge may mitigate the occurrence of blooms of non-siliceous algae and may strongly influence the Si budget and cycling because such porewater-derived Si can compensate for the dwindling Si flux from riverine sources due to human activity (i.e., dam construction, reservoirs).

## 5. Conclusions

Based on a  $^{222}\text{Rn}$  advection-diffusion model, porewater discharge ranged from  $7.4$  to  $25.8$  (mean:  $12.9 \pm 5.8$ )  $\text{cm d}^{-1}$  in a coastal aquifer of Shengsi Island. Its associated nutrient fluxes (DIN, DIP and DSi) were estimated to be  $(1.7 \pm 1.4) \times 10^{-2}$ ,  $(2.1 \pm 1.1) \times 10^{-4}$  and  $(1.5 \pm 1.3) \times 10^{-2} \text{ mol m}^{-2} \text{ d}^{-1}$ . Meanwhile, we found that the Si/N ratio of porewater ( $\sim 0.92$ ) in this study was higher than the Si/N ratio ( $\sim 0.68$ ) of river water in the Yangtze River Estuary, which may mitigate the occurrence of blooms of non-siliceous algae in the sea area near Shengsi Island. Our result may provide valuable information for effective management strategies of these vulnerable water resources in the

Zhoushan Fishing Ground (one of the ten largest fishing counties in China). In addition, considering that the decline in the Si flux from riverine input is due to human activity (i.e., dam construction, reservoirs), the Si flux with a higher Si/N ratio through porewater discharge like Shengsi Island may influence the global Si budget and cycling.

## Acknowledgements

We would like to thank all the colleagues of the radioisotope group from SKLEC/ECNU for their assistance in the field. We acknowledge the Editor Mike Elliott and three anonymous reviewers for their constructive comments that significantly improved the original manuscript. This research was supported by the Natural Science Foundation of China (Grant No. 41576083 and 41376089).

## References

- Benoit, J.M., Torgersen, T., O'Donnell, J., 1991. An advection/diffusion model for  $^{222}\text{Rn}$  transport in near-shore sediments inhabited by sedentary polychaetes. *Earth Planet. Sci. Lett.* 105 (4), 463–473.
- Bhadha, J.H., Martin, J.B., Jaeger, J., Lindenberg, M., Cable, J.E., 2007. Surface and pore water mixing in estuarine sediments: implications for nutrient and Si cycling. *J. Coast Res.* 23 (4), 878–891.
- Boehm, A.B., Paytan, A., Shellenberger, G.G., Davis, K.A., 2006. Composition and flux of groundwater from a California beach aquifer: implications for nutrient supply to the surf zone. *Cont. Shelf Res.* 26, 269–282.
- Burnett, W.C., Bokuniewicz, H., Huettel, M., Moore, W.S., Taniguchi, M., 2003. Groundwater and porewater inputs to the coastal zone. *Biogeochemistry* 66 (1–2), 3–33.
- Burnett, W.C., Dulaiova, H., 2006. Radon as a tracer of submarine groundwater discharge into a boat basin in Donnalucata, Sicily. *Cont. Shelf Res.* 26 (7), 862–873.
- Cable, J.E., Burnett, W.C., Chanton, J.P., Weatherly, G.L., 1996. Estimating groundwater discharge into the northeastern Gulf of Mexico using radon-222. *Earth Planet. Sci. Lett.* 144 (3), 591–604.
- Charette, M.A., Allen, M.C., 2006. Precision ground water sampling in coastal aquifers using a direct-push, shielded-screen well-point system. *Groundwater Monit. Remediat.* 26 (2), 87–93.
- Charette, M.A., Sholkovitz, E.R., 2006. Trace element cycling in a subterranean estuary: Part 2. Geochemistry of the pore water. *Geochem. Cosmochim. Acta* 70 (4), 811–826.
- Chen, T., Wang, Q.Q., Qin, Y., Chen, X., Yang, X.X., Lou, W., Zhou, M.K., He, G.X., Lu, K., 2015. Knowledge, Attitudes and practice of desalinated water among professionals in health and water departments in Shengsi, China: a qualitative study. *PLoS One* 10 (4), e0118360.
- Chen, X., Lao, Y., Wang, J., Du, J., Liang, M., Yang, B., 2018a. Submarine groundwater-borne nutrients in a tropical bay (Maowei Sea, China) and their impacts on the oyster aquaculture. *G-cubed* 19 (3), 932–951.
- Chen, X., Zhang, F., Lao, Y., Wang, X., Du, J., Santos, I.R., 2018b. Submarine groundwater discharge-derived carbon fluxes in mangroves: an important component of blue carbon budgets? *J. Geophys. Res. Oceans* 123 (9), 6962–6979.
- Cociasu, A., Dorogan, L., Humborg, C., Popa, L., 1996. Long-term ecological changes in

- the Romanian coastal waters of the Black Sea. *Mar. Pollut. Bull.* 32, 32–38.
- Craig, H., 1969. Abyssal carbon and radiocarbon in the Pacific. *J. Geophys. Res.* 74 (23), 5491–5506.
- Dai, Z., Du, J., Zhang, X., Su, N., Li, J., 2010. Variation of riverine material loads and environmental consequences on the Changjiang (Yangtze) Estuary in recent decades (1955–2008). *Environ. Sci. Technol.* 45 (1), 223–227.
- Dai, Z., Liu, J., 2013. Impacts of large dams on downstream fluvial sedimentation: an example of the three gorges dam (TGD) on the Changjiang (Yangtze River). *J. Hydrol.* 480, 10–18.
- Dale, A.W., Bertics, V.J., Treude, T., Sommer, S., Wallmann, K., 2013. Modeling benthic-pelagic nutrient exchange processes and porewater distributions in a seasonally hypoxic sediment: evidence for massive phosphate release by Beggiatoa? *Biogeosciences* 10 (2), 629–651.
- Dollar, S.J., Atkinson, M.J., 1992. Effects of nutrient subsidies from groundwater to nearshore marine ecosystems off the island of Hawaii. *Estuar. Coast Shelf Sci.* 35 (4), 409–424.
- Dür, H.H., Meybeck, M., Hartmann, J., Laruelle, G.G., Roubeix, V., 2011. Global spatial distribution of natural riverine silica inputs to the coastal zone. *Biogeosciences* 8 (3), 597–620.
- Faber, P.A., Evrard, V., Woodland, R.J., Cartwright, I.C., Cook, P.L., 2014. Pore-water exchange driven by tidal pumping causes alkalinity export in two intertidal inlets. *Limnol. Oceanogr.* 59 (5), 1749–1763.
- Glé, C., Del Amo, Y., Sautour, B., Laborde, P., Chardy, P., 2008. Variability of nutrients and phytoplankton primary production in a shallow macrotidal coastal ecosystem (Arcachon Bay, France). *Estuar. Coast Shelf Sci.* 76 (3), 642–656.
- Georg, R.B., West, A.J., Basu, A.R., Halliday, A.N., 2009. Silicon fluxes and isotope composition of direct groundwater discharge into the Bay of Bengal and the effect on the global ocean silicon isotope budget. *Earth Planet. Sci. Lett.* 283 (1), 67–74.
- Gu, H., Moore, W.S., Zhang, L., Du, J., Zhang, J., 2012. Using radium isotopes to estimate the residence time and the contribution of submarine groundwater discharge (SGD) in the Changjiang effluent plume, East China Sea. *Cont. Shelf Res.* 35, 95–107.
- Humborg, C., Ittekkot, V., Cociaus, A., von Bodungen, B., 1997. Effect of Danube River dam on black sea biogeochemistry and ecosystem structure. *Nature* 386, 385–388.
- Humborg, C., Conley, D.J., Rahm, L., Wulff, F., Cociaus, A., Ittekkot, V., 2000. Silicon retention in river basins: far-reaching effects on biogeochemistry and aquatic food webs in coastal marine environments. *Ambio* 29 (1), 45–50.
- Hwang, D.W., Lee, Y.W., Kim, G., 2005a. Large submarine groundwater discharge and benthic eutrophication in Bangdu Bay on volcanic Jeju Island, Korea. *Limnol. Oceanogr.* 50, 1393–1403.
- Hwang, D.W., Kim, G., Lee, Y.W., Yang, H.S., 2005b. Estimating submarine inputs of groundwater and nutrients to a coastal bay using radium isotopes. *Mar. Chem.* 96 (1), 61–71.
- Hwang, D.W., Lee, I.S., Choi, M., Kim, T.H., 2016. Estimating the input of submarine groundwater discharge (SGD) and SGD-derived nutrients in Geoje Bay, Korea using  $^{222}\text{Rn}$ -Si mass balance model. *Mar. Pollut. Bull.* 110 (1), 119–126.
- Kim, G., Ryu, J.W., Yang, H.S., Yun, S.T., 2005. Submarine groundwater discharge (SGD) into the Yellow Sea revealed by  $^{228}\text{Ra}$  and  $^{226}\text{Ra}$  isotopes: implications for global silicate fluxes. *Earth Planet. Sci. Lett.* 237 (1), 156–166.
- Lee, Y.W., Kim, G., Lim, W.A., Hwang, D.W., 2010. A relationship between submarine-groundwater borne nutrients traced by Ra isotopes and the intensity of dinoflagellate red-tides occurring in the southern sea of Korea. *Limnol. Oceanogr.* 55, 1–10.
- Liu, J., Su, N., Wang, X., Du, J., 2017. Submarine groundwater discharge and associated nutrient fluxes into the Southern Yellow Sea: a case study for semi-enclosed and oligotrophic seas-implication for green tide bloom. *J. Geophys. Res. Oceans* 122 (1), 139–152.
- Liu, J., Du, J., Wu, Y., Liu, S., 2018. Nutrient input through submarine groundwater discharge in two major Chinese estuaries: the Pearl River Estuary and the Changjiang River Estuary. *Estuar. Coast Shelf Sci.* 203, 17–28.
- Liu, S., Zhang, J., Chen, H., Zhang, G., 2005. Factors influencing nutrient dynamics in the eutrophic Jiaozhou Bay, North China. *Prog. Oceanogr.* 66, 66–85.
- Liu, S., Hong, G., Zhang, J., Ye, X., Jiang, X., 2009. Nutrient budgets for large Chinese estuaries. *Biogeosciences* 6, 2245–2263.
- Liu, S., Qi, X., Li, X., Ye, H., Wu, Y., Ren, J., Zhang, J., Xu, W., 2016. Nutrient dynamics from the Changjiang (Yangtze River) estuary to the East China sea. *J. Mar. Syst.* 154, 15–27.
- Luo, X., Jiao, J.J., 2016. Submarine groundwater discharge and nutrient loadings in Tolo Harbor, Hong Kong using multiple geotracer-based models, and their implications of red tide outbreaks. *Water Res.* 102, 11–31.
- Martens, C.S., Klump, J.V., Kipphut, G.W., 1980. Sediment-water chemical exchange in the coastal zone traced by in situ radon-222 flux measurements. *Science* 208 (4441), 285–288.
- Mayer, L.M., Gloss, S.P., 1980. Buffering of silica and phosphorus in a turbid river. *Limnol. Oceanogr.* 25, 12–22.
- McCoy, C., Viso, R., Peterson, R.N., Libes, S., Lewis, B., Ledoux, J., Voulgaris, G., Smith, E., Sanger, D., 2011. Radon as an indicator of limited cross-shelf mixing of submarine groundwater discharge along an open ocean beach in the South Atlantic Bight during observed hypoxia. *Cont. Shelf Res.* 31, 1306–1317.
- Meybeck, M., Helmer, R., 1989. The quality of rivers: from pristine stage to global pollution. *Global Planet. Change* 1 (4), 283–309.
- Moore, W.S., 2010. The effect of submarine groundwater discharge on the ocean. *Ann. Rev. Mar. Sci.* 2, 59–88.
- Nolan, B.T., Hitt, K.J., Ruddy, B.C., 2002. Probability of nitrate contamination of recently recharged groundwaters in the conterminous United States. *Environ. Sci. Technol.* 36 (10), 2138–2145.
- O'Reilly, C., Santos, I.R., Cyronak, T., McMahon, A., Maher, D.T., 2015. Nitrous oxide and methane dynamics in a coral reef lagoon driven by pore water exchange: insights from automated high-frequency observations. *Geophys. Res. Lett.* 42 (8), 2885–2892.
- Peng, T.H., Takahashi, T., Broecker, W.S., 1974. Surface radon measurements in the north Pacific ocean station PAPA. *J. Geophys. Res.* 79 (12), 1772–1780.
- Santos, I.R., Burnett, W.C., Misra, S., Suryaputra, I.G.N.A., Chanton, J.P., Dittmar, T., Peterson, R.N., Swarzenski, P.W., 2011. Uranium and barium cycling in a salt wedge subterranean estuary: the influence of tidal pumping. *Chem. Geol.* 287 (1), 114–123.
- Santos, I.R., Eyre, B.D., Huettel, M., 2012. The driving forces of porewater and groundwater flow in permeable coastal sediments: a review. *Estuar. Coast Shelf Sci.* 98, 1–15.
- Santos, I.R., Beck, M., Brumsack, H.J., Maher, D.T., Dittmar, T., Waska, H., Schnetger, B., 2015. Porewater exchange as a driver of carbon dynamics across a terrestrial-marine transect: insights from coupled  $^{222}\text{Rn}$  and  $\text{pCO}_2$  observations in the German Wadden Sea. *Mar. Chem.* 171, 10–20.
- Slomp, C.P., Van Cappellen, P., 2004. Nutrient inputs to the coastal ocean through submarine groundwater discharge: controls and potential impact. *J. Hydrol.* 295 (1), 64–86.
- Smith, C.G., Cable, J.E., Martin, J.B., Roy, M., 2008. Evaluating the source and seasonality of submarine groundwater discharge using a radon-222 pore water transport model. *Earth Planet. Sci. Lett.* 273 (3), 312–322.
- Sugimoto, R., Honda, H., Kobayashi, S., Takao, Y., Tahara, D., Tominaga, O., Taniguchi, M., 2016. Seasonal changes in submarine groundwater discharge and associated nutrient transport into a tideless semi-enclosed embayment (Obama Bay, Japan). *Estuar. Coast* 39 (1), 13–26.
- Su, N., Du, J., Moore, W.S., Liu, S., Zhang, J., 2011. An examination of groundwater discharge and the associated nutrient fluxes into the estuaries of eastern Hainan Island, China using  $^{226}\text{Ra}$ . *Sci. Total Environ.* 409 (19), 3909–3918.
- Swarzenski, P.W., Reich, C., Kroeger, K.D., Baskaran, M., 2007. Ra and Ru isotopes as natural tracers of submarine groundwater discharge in Tampa Bay, Florida. *Mar. Chem.* 104 (1), 69–84.
- Tait, D.R., Maher, D.T., Sanders, C.J., Santos, I.R., 2017. Radium-derived porewater exchange and dissolved N and P fluxes in mangroves. *Geochem. Cosmochim. Acta* 200, 295–309.
- Taniguchi, M., Burnett, W.C., Cable, J.E., Turner, J.V., 2002. Investigation of submarine groundwater discharge. *Hydrog. Process.* 16 (11), 2115–2129.
- Teodoru, C., Dimopoulos, A., Wehrli, B., 2006. Biogenic silica accumulation in the sediments of iron gate I reservoir on the Danube River. *Aquat. Sci.* 68 (4), 469–481.
- Trégouer, P.J., De La Rocha, C.L., 2013. The world ocean silica cycle. *Ann. Rev. Mar. Sci.* 5, 477–501.
- Trégouer, P., Nelson, D.M., Van Bennekom, A.J., DeMaster, D.J., Leynaert, A., Quégúiner, B., 1995. The silica balance in the world ocean: a reestimate. *Science* 268, 375–379.
- Ullman, W.J., Aller, R.C., 1982. Diffusion coefficients in nearshore marine sediments. *Limnol. Oceanogr.* 27 (3), 552–556.
- Urquidi-Gaume, M., Santos, I.R., Lechuga-Devez, C., 2016. Submarine groundwater discharge as a source of dissolved nutrients to an arid coastal embayment (La Paz, Mexico). *Environ. Earth Sci.* 75 (2), 154.
- Valiela, I., Costa, J., Foreman, K., Teal, J.M., Howes, B., Aubrey, D., 1990. Transport of groundwater-borne nutrients from watersheds and their effects on coastal waters. *Biogeochemistry* 10, 177–197.
- Wahby, S.D., Bishara, N.F., 1981. The effect of the river nile on Mediterranean water, before and after the construction of the high dam at Aswan. In: Martin, J.-M., Burton, J.D., Eisma, D. (Eds.), *River Inputs to Ocean Systems*. UNEP, IOC, SCOR, United Nations, New York, pp. 311–318.
- Wang, G., Wang, Z., Zhai, W., Moore, W.S., Li, Q., Yan, X., Qi, D., Jiang, Y., 2015. Net subterranean estuarine export fluxes of dissolved inorganic C, N, P, Si, and total alkalinity into the Jiulong River estuary, China. *Geochem. Cosmochim. Acta* 149, 103–114.
- Wang, W., Cao, X., Yuan, Y., Song, X., Yu, Z., 2016. Variation and controlling factor of nutrient distribution in Changjiang River Estuary and adjacent areas in 2012. *Oceanol. Limnol. Sinica* 47 (4), 804–812 (in Chinese with English abstract).
- Wang, X., Li, H., Yang, J., Zheng, C., Zhang, Y., An, A., Zhang, M., Xiao, K., 2017. Nutrient inputs through submarine groundwater discharge in an embayment: a radon investigation in Daya Bay, China. *J. Hydrol.* 551, 784–792.
- Wang, X., Du, J., 2016. Submarine groundwater discharge into typical tropical lagoons: a case study in eastern Hainan Island, China. *G-cubed* 17 (11), 4366–4382.
- Wang, X., Baskaran, M., Su, K., Du, J., 2018. The important role of submarine groundwater discharge (SGD) to derive nutrient fluxes into River dominated Ocean Margins-The East China Sea. *Mar. Chem.* 204, 121–132.
- Wen, T., Du, J., Ji, T., Wang, L., Deng, B., 2014. Use of  $^{222}\text{Rn}$  to trace submarine groundwater discharge in a tidal period along the coast of Xiangshan, Zhejiang, China. *J. Radioanal. Nucl. Chem.* 299 (1), 53–60.
- Wu, Z., Zhou, H., Zhang, S., Liu, Y., 2013. Using  $^{222}\text{Rn}$  to estimate submarine groundwater discharge (SGD) and the associated nutrient fluxes into Xiangshan Bay, East China Sea. *Mar. Pollut. Bull.* 73 (1), 183–191.
- Yang, S.L., Zhang, J., Zhu, J., Smith, J.P., Dai, S.B., Gao, A., Li, P., 2005. Impact of dams on Yangtze River sediment supply to the sea and delta intertidal wetland response. *J. Geophys. Res.* 110<sup>https://doi.org/10.1029/2004JF000271</sup>. (F03006).
- Yang, Z.S., Wang, H.J., Saito, Y., Milliman, J.D., Xu, K., Qiao, S., Shi, G., 2006. Dam impacts on the Changjiang (Yangtze) river sediment discharge to the sea: the past 55 years and after the three gorges dam. *Water Resour. Res.* 42 (4). <sup>https://doi.org/10.1029/2005WR003970</sup>.
- Zhang, G., Zhang, J., Liu, S., 2007a. Characterization of nutrients in the atmospheric wet and dry deposition observed at the two monitoring sites over Yellow Sea and East China Sea. *J. Atmos. Chem.* 57 (1), 41–57.
- Zhang, J., Yu, B., 2001. The phytoplankton and the red tide monitoring in Yangtze Estuary and Shengshi Islands. *J. Zhejiang Ocean Univ. (Nat. Sci.)* 20 (3), 213–216 (in Chinese with English abstract).
- Zhang, J., Liu, S., Ren, J., Wu, Y., Zhang, G., 2007b. Nutrient gradients from the eutrophic Changjiang (Yangtze River) estuary to the oligotrophic Kuroshio waters and re-evaluation of budgets for the East China sea shelf. *Prog. Oceanogr.* 74 (4), 449–478.
- Zhou, M., Shen, Z., Yu, R., 2008. Responses of a coastal phytoplankton community to increased nutrient input from the Changjiang (Yangtze) River. *Cont. Shelf Res.* 28 (12), 1483–1489.